Mycological Progress (2019) 18:593–602
https://doi.org/10.1007/s11557-019-01472-8

DGfM

ORIGINAL ARTICLE

Two new *Neofomitella* species (Polyporaceae, Basidiomycota) based on morphological and molecular evidence

Xing Ji[1] · Dong-Mei Wu[2] · Chang-Ge Song[1] · Shun Liu[1] · Jing Si[1] · Bao-Kai Cui[1]

Received: 6 December 2018 / Revised: 10 January 2019 / Accepted: 13 January 2019

Abstract

Two new *Neofomitella* species, *N. australiensis* and *N. guangxiensis*, are described based on morphological and molecular characters. *Neofomitella australiensis* is characterized by white pore surface when fresh, dextrinoid skeletal and binding hyphae, and orange-red context near pileal surface when fresh. *Neofomitella guangxiensis* is characterized by round to angular pores (5–6 per mm), weakly dextrinoid skeletal and binding hyphae and large basidiospores (5.5–7.5 × 1.8–2.2 μm). Phylogenetic analyses were carried out based on sequences from the internal transcribed spacer (ITS), the large subunit nuclear ribosomal RNA gene (nLSU), the small subunit nuclear ribosomal RNA gene (nSSU), the small subunit mitochondrial rRNA gene (mtSSU), the translation elongation factor 1-α gene (EF1-α), the largest subunit of RNA polymerase II (RPB1) and the second largest subunit of RNA polymerase II (RPB2), and the result confirmed the affinities of the two new species within *Neofomitella*. An identification key to species of *Neofomitella* is provided.

Keywords Multi-locus analysis · Phylogeny · Polyporaceae · Taxonomy · Wood-rotting fungi

Introduction

Neofomitella Y.C. Dai, Hai J. Li & Vlasák (Polyporaceae, Polyporales) was recently derived from *Fomitella* Murrill and typified by *N. rhodophaea* (Lév.) Y.C. Dai, Hai J. Li & Vlasák, it differs from *Fomitella* by its distinctly crusted basidiomata with the cuticle developing from base to margin (Li et al. 2014). Species in *Neofomitella* have annual or perennial growth habit; pileate or effused-reflexed basidiomata; concentrically zonate or sulcate and glabrous to velutinate pileal surface; corky to hard corky context with a dark agglutinated crust developing from base to margin; and a trimitic hyphal system with clamped generative hyphae, tissues turning to black in KOH, oblong ellipsoid to cylindrical, hyaline, smooth and thin-walled basidiospores (Li et al. 2014). Phylogenetic analysis showed that *Neofomitella* clustered with *Microporus* P. Beauv., with no close relationships to *Fomitella* (Li et al. 2014). Currently, three species are accepted in *Neofomitella*: *N. rhodophaea*; *N. fumosipora* (Corner) Y.C. Dai, Hai J. Li & Vlasák; and *N. polyzonata* Y.C. Dai, Hai J. Li & Vlasák.

During the investigations on species diversity and taxonomy of polypores, two undescribed taxa matching the definitions of *Neofomitella* were found. In order to confirm the affinity of these taxa with the *Neofomitella* species, phylogenetic analysis was carried out based on a combined 7-gene dataset.

Section Editor: Marc Stadler

✉ Bao-Kai Cui
baokaicui2013@gmail.com

[1] Institute of Microbiology, Beijing Forestry University, Beijing 100083, China

[2] Biotechnology Research Institute, Xinjiang Academy of Agricultural and Reclamation Sciences, Xinjiang Production & Construction Group Key Laboratory of Crop Germplasm Enhancement and Gene Resources Utilization, Shihezi 832000, Xinjiang, China

Materials and methods

Morphological studies

The examined specimens were deposited at the herbarium of the Institute of Microbiology, Beijing Forestry University (BJFC), and some duplicates were deposited at the herbarium of Royal Botanic Gardens Victoria, Australia (MEL). Macromorphological descriptions were based on the field notes and measurements of herbarium specimens. Color terms followed

Petersen (1996). Micro-morphological data were obtained from the dried specimens, and observed under a light microscope following Han et al. (2016) and Shen et al. (2019). Sections were studied at a magnification of up to × 1000 using a Nikon E 80i microscope and phase contrast illumination. Drawings were made with the aid of a drawing tube. Microscopic features, measurements, and drawings were made from slide preparations stained with Cotton Blue and Melzer's reagent. Spores were measured from sections cut from the tubes. To present the variation of spore size, 5% of measurements excluded from each end of the range were given in parentheses. The following abbreviations were used: IKI = Melzer's reagent, IKI– = neither amyloid nor dextrinoid, CB = cotton blue, CB– = acyanophilous, KOH = 5% potassium hydroxide, L = mean spore length (arithmetic average of all spores), W = mean spore width (arithmetic average of all spores), Q = variation in the L/W ratios between the specimens studied, n (a/b) = number of spores (a) measured from given number (b) of specimens.

DNA extraction and sequencing

A CTAB rapid plant genome extraction kit (Aidlab Biotechnologies Co. Ltd., Beijing) was used to extract total genomic DNA from dried specimens, and performed the polymerase chain reaction (PCR) according to the manufacturer's instructions with some modifications (Chen et al. 2015; Zhou et al. 2016). The ITS region was amplified with primer pairs ITS5 and ITS4 (White et al. 1990). The nLSU region was amplified with primer pairs LR0R and LR7 (http://www.biology.duke.edu/fungi/mycolab/primers.htm). The nSSU region was amplified with primer pairs PNS1 and NS41 (Hibbett 1996). The mtSSU region was amplified with primer pairs MS1 and MS2 (White et al. 1990). Part of EF1-α was amplified with primer pairs EF1-983F and EF1-1567R (Rehner and Buckley 2005). RPB1 was amplified with primer pairs RPB1-Af and RPB1-Cr (Matheny et al. 2002). RPB2 was amplified with primer pairs fRPB2-5F and fRPB2-7cR (Liu et al. 1999). The PCR procedure for ITS, mtSSU, and EF1-α included an initial denaturation at 95 °C for 3 min, followed by 34 cycles at 94 °C for 40 s, 54 °C for ITS and mtSSU, 56 °C for EF1-α for 45 s, 72 °C for 1 min, and a final extension of 72 °C for 10 min. The PCR procedure for nLSU and nSSU included an initial denaturation at 94 °C for 1 min, followed by 34 cycles at 94 °C for 30 s, 50 °C for nLSU and 53 °C for nSSU for 1 min, 72 °C for 1.5 min, and a final extension of 72 °C for 10 min. The PCR procedure for RPB1 and RPB2 included an initial denaturation at 94 °C for 2 min, followed by 10 cycles at 94 °C for 40 s, 60 °C for 40 s and 72 °C for 2 min, then followed by 37 cycles at 94 °C for 45 s, 53 °C–58 °C for 1.5 min and 72 °C for 2 min, and a final extension of 72 °C for 10 min. The PCR products were purified and sequenced at Beijing Genomics Institute, China, with the same primers. All newly generated sequences were submitted to GenBank and listed in Table 1.

Phylogenetic analyses

Additional sequences were selected from GenBank (Table 1). All sequences were aligned in MAFFT 7 (Katoh and Standley 2013; http://mafft.cbrc.jp/alignment/server/) and manually adjusted in BioEdit (Hall 1999). These gene fragments were spliced with Mesquite 3.2 (Maddison and Maddison 2017) for further phylogenetic analyses. The final concatenated sequence alignment was deposited in TreeBase (https://treebase.org/treebase-web/home.html; submission ID 23613). Sequences of *Laetiporus montanus* Černý ex Tomšovský & Jankovský and *L. sulphureus* (Bull.) Murrill were used as outgroups to root trees.

Maximum parsimony (MP) analysis was applied to the combined multiple genes datasets, and the tree construction procedure was performed in PAUP* version 4.0b10 (Swofford 2002). Settings for phylogenetic analyses followed Song et al. (2016) and Song and Cui (2017). All characters were equally weighted and gaps were treated as missing data. Trees were inferred using the heuristic search option with TBR branch swapping and 1000 random sequence additions. Maxtrees were set to 5000; branches of zero length were collapsed and all parsimonious trees were saved. Clade robustness was assessed using a bootstrap (BT) analysis with 1000 replicates (Felsenstein 1985). Descriptive tree statistics tree length (TL), consistency index (CI), retention index (RI), rescaled consistency index (RC), and homoplasy index (HI) were calculated for each maximum parsimonious tree (MPT) generated.

RAxML v7.2.6 (Stamatakis 2006) was used to construct a maximum likelihood (ML) tree involved 200 ML searches under the GTR+GAMMA model and only the best tree from all searches was kept. In addition, 200 rapid bootstrap replicates were run with the GTR+CAT model to obtain the ML bootstrap values.

MrModeltest 2.3 (Posada and Crandall 1998; Nylander 2004) was used to determine the best-fit evolution model for the combined dataset for Bayesian inference (BI). Bayesian inference (BI) was calculated with MrBayes v3.1.2 (Ronquist and Huelsenbeck 2003) with a general time reversible (GTR) model of DNA substitution and a gamma distribution rate variation across sites. Four Markov chains were run for two runs from random starting trees for 2 million generations and sampled every 100 generations. The first quarter generations were discarded as burn-in. A majority rule consensus tree of all remaining trees was calculated.

Phylogenetic trees were visualized using FigTree v1.4.2 (http://tree.bio.ed.ac.uk/software/figtree/). Branches that received bootstrap support for maximum parsimony (MP), maximum likelihood (ML) and Bayesian posterior

Table 1 A list of species, specimens and GenBank accession numbers of sequences used in this study

Species	Sample no.	GenBank accessions						
		ITS	nLSU	mtSSU	EF1-α	RPB1	RPB2	nSSU
Abundisporus fuscopurpureus	Cui 10969	KC456255	KC456257	KF051026	KF181155	–	–	MG847239
A. violaceus	Ryvarden 32807	KF018127	KF018135	KF051038	KF181132	–	–	–
Coriolopsis aspera	Cui 6702	KC867353	KC867476	–	–	–	KF274658	–
C. aspera	Cui 6725	KC867356	KC867477	–	–	–	KF274659	–
C. glabro-rigens	Dai 7894	KC867395	–	KX838375	–	–	–	–
C. glabro-rigens	Cui 13868	MK192427[a]	MK192446[a]	MK192466[a]	–	MK192505[a]	MK204694[a]	MK192485[a]
C. polyzona	BKW004	JN164978	JN164790	–	JN164881	JN164844	JN164856	–
C. rigida	BJFC12680	KC867381	KC867454	–	–	–	KF274664	–
C. rigida	JV0904_151	JF894113	–	–	–	–	–	–
C. sanguinaria	Dai 9362	KC867391	KC867466	KX838377	–	–	–	–
C. sanguinaria	Cui 14507	MK192428[a]	MK192447[a]	MK192467[a]	MK192519[a]	MK192506[a]	MK204695[a]	MK192486[a]
C. strumosa	Cui 14237	MK192429[a]	MK192448[a]	MK192468[a]	MK192520[a]	MK192507[a]	MK204696[a]	MK192487[a]
C. strumosa	Cui 16811	–	MK192449[a]	MK192469[a]	MK192521[a]	–	MK204697[a]	MK192488[a]
Daedaleopsis sinensis	Dai 11429	KU892444	KU892446	KX838383	KX838420	KU892476	KU892493	–
D. tricolor	Dai 8349	KU892432	KU892470	KX838385	KX838422	KU892490	KU892501	–
Earliella scabrosa	PR1209	JN165009	JN164793	–	JN164894	JN164819	JN164866	–
Fomes fomentarius	ES 2008-3	JX109860	JX109860	–	–	–	–	–
Fomitella supina	JV0610	KF274645	KF274646	–	–	–	–	–
F. supina	Ryvarden 39027	KF274643	–	–	–	–	–	–
Funalia gallica	RLG-7630-sp	JN165013	JN164814	–	–	JN164821	JN164869	–
F. gallica	FP91663T	JN165012	–	–	–	JN164845	JN164868	–
F. subgallica	Cui 6317	KC867384	KC867460	MG847226	MG867695	MG867665	KU182650	MG847242
F. subgallica	Dai 10741	KC867385	KC867461	MG847227	MG867696	MG867666	KU182647	MG847243
F. trogii	RLG-4286-Sp	JN164993	JN164808	–	JN164898	JN164820,	JN164867	–
F. trogii	KUC3030	DQ912696	AY858359	–	–	–	–	–
F. trogii	Dai 11246	KC867380	KC867451	KX838400	KX838432	KX838468	KU182653	–
Hexagonia apiaria	Cui 16818	MK192430[a]	MK192450[a]	MK192470[a]	MK192522[a]	MK192508[a]	MK204698[a]	MK192489[a]
H. apiaria	Dai 10784	KX900635	KX900682	KX900732	KX900822	MG867668	MG867677	MG847245
H. glabra	Cui 11367	KX900638	KX900684	KX900734	KX900824	MG867669	KX900798	MG847247
H. glabra	Cui 16796	MK192431[a]	MK192451[a]	–	MK192523[a]	MK192509[a]	MK204699[a]	MK192490[a]
Laetiporus montanus	Cui 10011	KF951274	KF951315	KX354570	KX354617	MG867670	KT894790	KX354528
L. sulphureus	Cui 12388	KR187105	KX354486	KX354560	KX354607	MG867671	KX354652	KX354518
Lenzites betulina	HHB-9942-Sp	JN164983	JN164794	–	JN164895	JN164822	JN164860	–
Megasporia hexagonoides	Cui 13855	MG847209	MG847218	MG847230	MG867701	–	MG867681	MG847255

Table 1 (continued)

Species	Sample no.	GenBank accessions						
		ITS	nLSU	mtSSU	EF1-α	RPB1	RPB2	nSSU
M. violacea	Cui 13838	MG847210	MG847219	MG847231	MG867702	–	MG867682	MG847256
Microporus affinis	Cui 7714	JX569739	JX569746	KX880696	–	–	KF274661	–
M. flabelliformis	Dai 11574	JX569740	JX569747	–	–	–	KF274662	–
M. vernicipes	Dai 9283	KX880618	KX880658	KX880701	KX880926	–	–	–
M. xanthopus	Cui 8284	JX290074	JX290071	KX880703	KX880878	–	JX559313	–
Neofomitella australiensis	Cui 16542	MK192438[a]	MK192458[a]	MK192477[a]	MK192530[a]	MK192511[a]	MK204706[a]	MK192497[a]
N. australiensis	Cui 16543	MK192439[a]	MK192459[a]	MK192478[a]	MK192531[a]	MK192512[a]	MK204707[a]	MK192498[a]
N. australiensis	Cui 16558	MK192440[a]	MK192460[a]	MK192479[a]	MK192532[a]	MK192513[a]	MK204708[a]	MK192499[a]
N. australiensis	Cui 16561	MK192441[a]	MK192461[a]	MK192480[a]	–	MK192514[a]	MK204709[a]	MK192500[a]
N. australiensis	Cui 16570	MK192442[a]	MK192462[a]	MK192481[a]	–	MK192515[a]	MK204710[a]	MK192501[a]
N. australiensis	Cui 16571	MK192443[a]	MK192463[a]	MK192482[a]	MK192533[a]	MK192516[a]	MK204711[a]	MK192502[a]
N. australiensis	Cui 16642	MK192444[a]	MK192464[a]	MK192483[a]	MK192534[a]	MK192517[a]	–	MK192503[a]
N. australiensis	Cui 16679	MK192445[a]	MK192465[a]	MK192484[a]	–	MK192518[a]	–	MK192504[a]
N. fumosipora	Cui 8816	JX569734	JX569741	KX900766	–	–	–	–
N. fumosipora	Cui 16750	MK192432[a]	MK192452[a]	MK192471[a]	MK192524[a]	MK192510[a]	MK204700[a]	MK192491[a]
N. fumosipora	Cui 16759	MK192433[a]	MK192453[a]	MK192472[a]	MK192525[a]	–	MK204701[a]	MK192492[a]
N. fumosipora	Dai 10777	JX569735	JX569742	–	–	–	–	–
N. guangxiensis	Cui 13968	MK192434[a]	MK192454[a]	MK192473[a]	MK192526[a]	–	MK204702[a]	MK192493[a]
N. guangxiensis	Cui 13984	MK192435[a]	MK192455[a]	MK192474[a]	MK192527[a]	–	MK204703[a]	MK192494[a]
N. guangxiensis	Cui 14005	MK192436[a]	MK192456[a]	MK192475[a]	MK192528[a]	–	MK204704[a]	MK192495[a]
N. guangxiensis	Cui 14029	MK192437[a]	MK192457[a]	MK192476[a]	MK192529[a]	–	MK204705[a]	MK192496[a]
N. polyzonata	Dai 10419	JX569738	JX569745	–	–	–	KF274663	–
N. polyzonata	Dai 10420	JX569736	JX569743	–	–	–	–	–
N. rhodophaea	TFRI 414	EU232216	EU232300	–	–	–	–	–
Pycnoporus sanguineus	PR-SC-95	JN164982	JN164795	–	JN164897	JN164842	JN164858	–
Trametes conchifer	FP-106793-Sp	JN164924	JN164797	–	JN164887	JN164823	JN164849	–
T. ochracea	HHB-13445-Sp	JN164954	JN164812	–	JN164904	JN164826	JN164852	–
T. versicolor	FP-135156-Sp	JN164919	JN164809	–	JN164878	JN164825	JN164850	–
Whitfordia scopulosa	Dai 10739	KC867364	KC867482	KX880766	KX880922	MG867675	MG867692	MG847272

[a] New sequences for this study

probabilities (BPP) greater than or equal to 75% (MP and ML) and 0.95 (BPP) were considered as significantly supported, respectively.

Results

Molecular phylogeny

The combined dataset (ITS+nLSU+mtSSU+nSSU+EF1-α+RPB1+RPB2) included sequences of 63 fungal specimens representing 37 taxa. The dataset had an aligned length of 6528 characters, of which 4464 characters are constant, 235 are variable and parsimony-uninformative, and 1829 are parsimony-informative. MP analysis yielded 40 equally parsimonious trees (TL = 7826, CI = 0.440, RI = 0.735, RC = 0.323, HI = 0.560). The best model for the combined dataset estimated and applied in the BI was GTR + I + G, lset nst = 6, rates = invgamma; prset statefreqpr = dirichlet (1,1,1,1). Bayesian and ML analyses resulted in a similar topology as MP analysis, with an average standard deviation of split frequencies = 0.003063 (BI); and the ML topology was shown in Fig. 1.

Samples of *Neofomitella* clustered together, then grouped with the samples of *Microporus* P. Beauv.

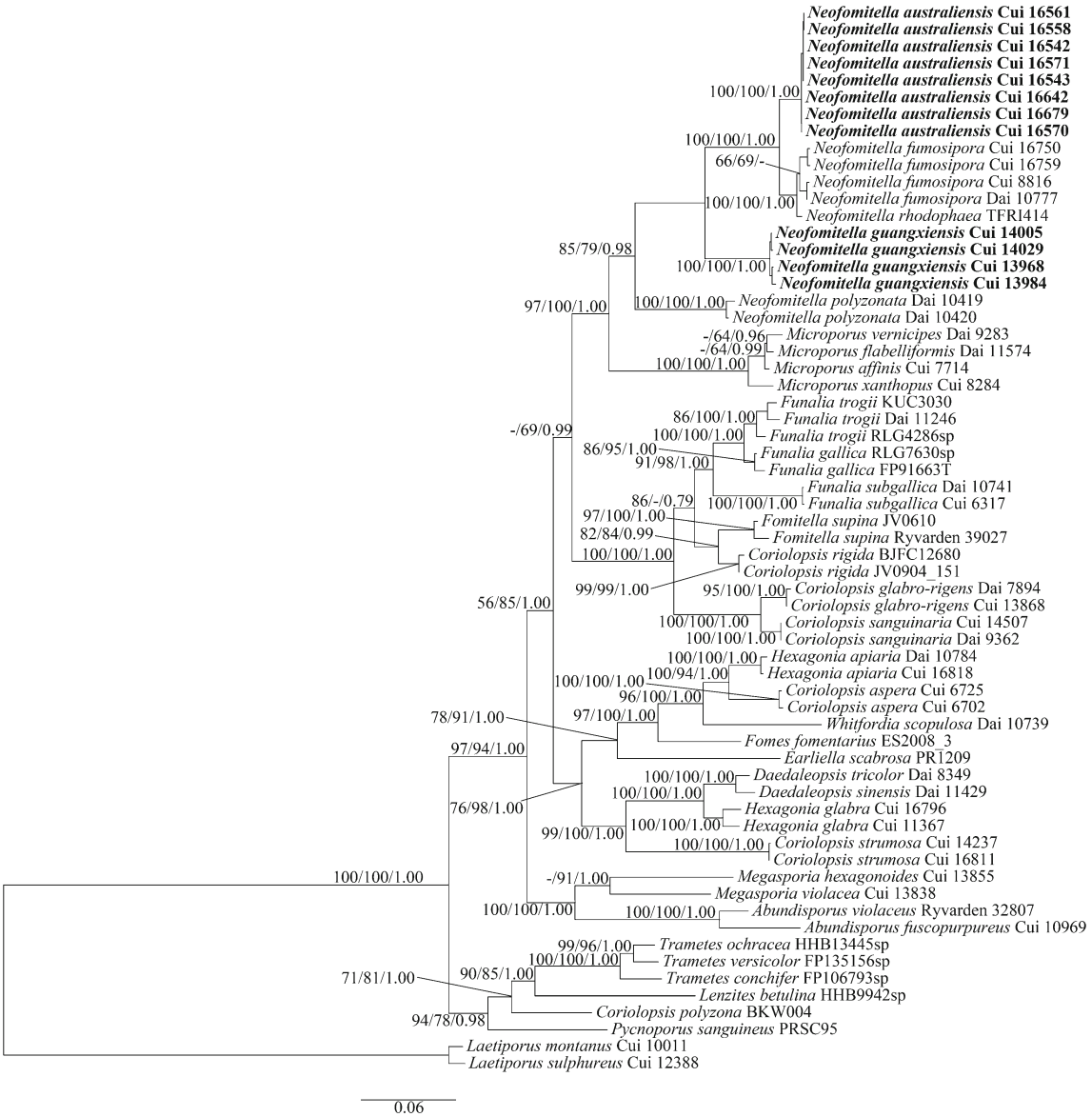

Fig. 1 Strict consensus tree illustrating the phylogeny of *Neofomitella* generated by ML analysis based on ITS+nLSU+mtSSU+nSSU+EF1-α+RPB1+RPB2 sequences. Branches are labeled with parsimony bootstrap proportions higher than 50%, maximum likelihood bootstrap higher than 50% and Bayesian posterior probabilities more than 0.95

Sampled specimens of the two new species formed distinctly well-supported lineages (Fig. 1).

Taxonomy

Neofomitella australiensis **B.K. Cui & Xing Ji, sp. nov.** (Figs. 2a–b, 3)

MycoBank: MB 828729

Diagnosis. Differs from other *Neofomitella* species by its distinctly pileate basidiomata, white pore surface when fresh, dextrinoid skeletal and binding hyphae, and presence of orange-red colored context close to the pileal surface when fresh.

Holotype. Australia. Victoria, Yarra Ranges National Park, on dead tree of *Nothofagus*, 10 May 2018, Cui 16,571 (BJFC, isotype in MEL).

Etymology. Australiensis (Lat.): referring to the locality (Australia) of the type specimens.

Basidiomata. Annual to perennial, pileate, sessile, hard corky, without odor or taste when fresh, woody hard upon drying. Pilei flabelliform or semicircular, sometimes ungulate, projecting up to 10 cm, 20 cm wide, and 8 cm thick at base. Pileal surface buff, grayish-brown, yellowish-brown to umber, glabrous, concentrically sulcate with different colored zones, margin obtuse. Pore surface white when fresh, becoming buff to cinnamon-buff when dry; sterile margin distinct, buff, up to 2 mm wide; pores round to angular, 6–7 per mm; dissepiments moderate thick to thick, entire. Context cream when fresh, buff upon drying, presence of an orange red line near pileal surface when fresh, which becoming cinnamon upon drying, woody hard, up to 6 cm thick. Tubes concolorous with context, hard corky, up to 2 cm long.

Hyphal structure. Hyphal system trimitic; generative hyphae bearing clamp connections; skeletal and binding hyphae dextrinoid, CB–; tissues unchanged in KOH.

Context. Generative hyphae in infrequent, hyaline, thin-walled, unbranched, 1.6–2.8 μm in diam; skeletal hyphae dominant, pale yellowish brown, thick-walled with a narrow lumen to subsolid, unbranched, more or less regularly arranged, 2.8–5.2 μm in diam; binding hyphae pale yellowish brown, thick-walled with a narrow lumen to subsolid, flexuous, frequently branched, interwoven, 1.2–2.4 μm in diam.

Tubes. Generative hyphae infrequent, hyaline, thin-walled, occasionally branched, 1.4–2.3 μm in diam; skeletal hyphae dominant, pale yellowish brown, thick-walled with a narrow lumen to subsolid, unbranched, interwoven, 2.2–4.3 μm in diam; binding hyphae hyaline to pale yellowish brown, thick-walled with a narrow lumen to subsolid, flexuous, frequently branched, interwoven, 0.7–2.2 μm in diam. Cystidia absent, fusoid cystidioles present, hyaline, thin-walled, 9.8–14.7 × 2.8–4.2 μm. Basidia clavate, bearing four sterigmata and a basal clamp connection, 10.2–15 × 4.4–5.3 μm; basidioles in shape similar to basidia, but slightly smaller.

Spores. Basidiospores cylindrical, hyaline, thin-walled, smooth, IKI–, CB–, (3.7–)3.8–4.9(−5.2) × (1.7–)1.8–2.3(−2.5) μm, $L = 4.2$ μm, $W = 2.02$ μm, $Q = 2.04–2.12$ ($n = 90/3$).

Fig. 2 Basidiomata of *Neofomitella* species. **a**, **b** *N. australiensis*; **c**, **d** *N. guangxiensis* (scale bars: **a**–**b** = 3 cm; **c**–**d** = 2 cm)

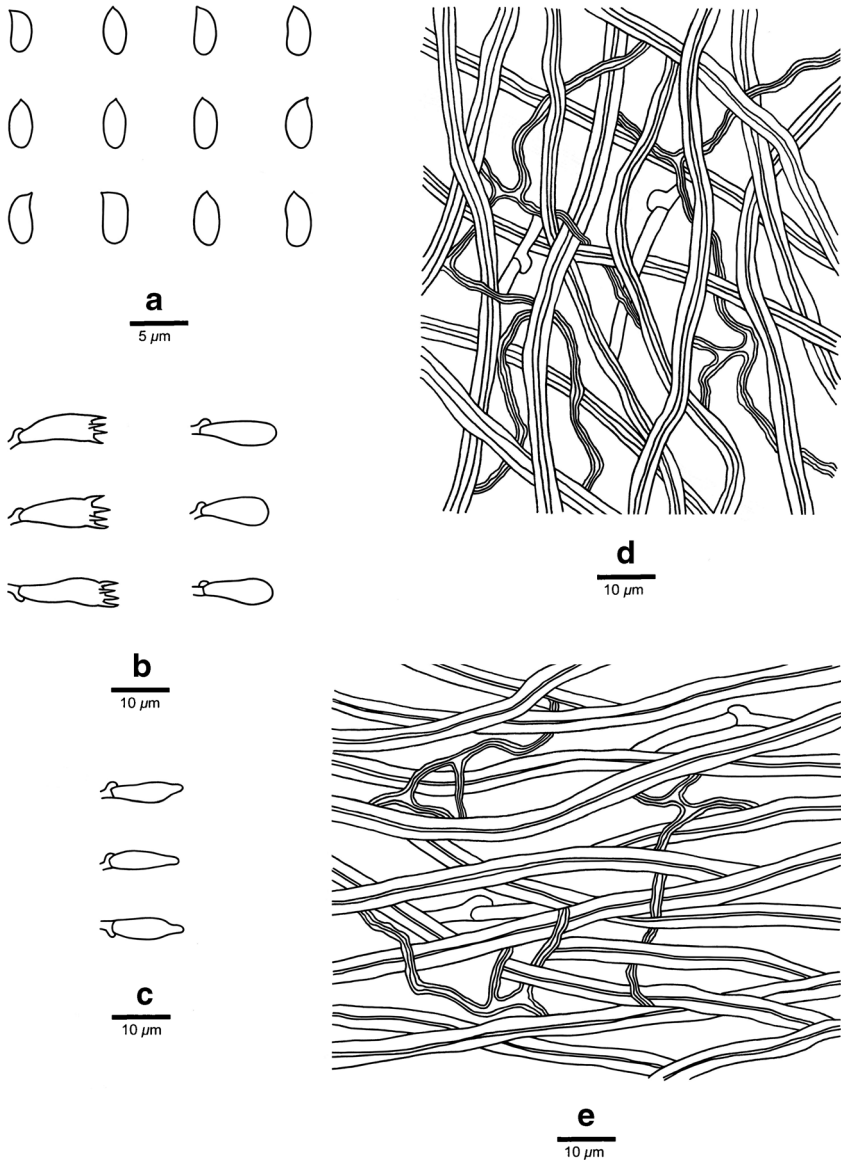

Fig. 3 Microscopic structures of *Neofomitella australiensis* (drawn from the holotype). **a** Basidiospores; **b** Basidia and basidioles; **c** Cystidioles; **d** Hyphae from trama; **e** Hyphae from context. Bars: **a** = 5 μm; **a**–**e** = 10 μm

Type of rot. White rot.

Additional specimens (paratypes) examined. Australia. Victoria, Yarra Ranges National Park, on fallen trunk of *Eucalyptus*, 10 May 2018, Cui 16542 & Cui 16543 (BJFC, duplicates in MEL). Victoria, Yarra Ranges National Park, on living tree of *Nothofagus*, 10 May 2018, Cui 16558, Cui16561 & Cui 16570 (BJFC, duplicates in MEL). Tasmania, on living tree of *Eucalyptus*, 10 May 2018, Cui 16642 & Cui 16679 (BJFC).

***Neofomitella guangxiensis* B.K. Cui & Xing Ji, sp. nov.** (Figs. 2c–d, 4).

MycoBank: MB 828730

Diagnosis. Differs from other *Neofomitella* species by its effused-reflexed to pileate basidiomata, round to angular pores (5–6 per mm), weakly dextrinoid skeletal and binding hyphae, and large basidiospores (5.5–7.5 × 1.8–2.2 μm).

Holotype. China. Guangxi Auto. Reg., Shangsi County, Shiwandashan National Forest Park, on fallen angiosperm branch, 6 July 2016, Cui 14029 (BJFC).

Etymology. Guangxiensis (Lat.): referring to the locality (Guangxi Auto. Reg.) of the type specimens.

Basidiomata. Annual, effused-reflexed to pileate, corky, without odor or taste when fresh, corky to hard corky upon drying. Pilei semicircular, projecting up to 1 cm, 3 cm wide, and 3 mm thick at base; up to 12.5 cm long, 3.5 cm wide, and 3 mm thick in the resupinate parts. Pileal surface straw-yellow, glabrous, concentrically sulcate, margin acute. Pore surface cream to clay-pink when fresh, becoming straw-yellow to clay-buff when dry; sterile margin indistinct, cream, up to

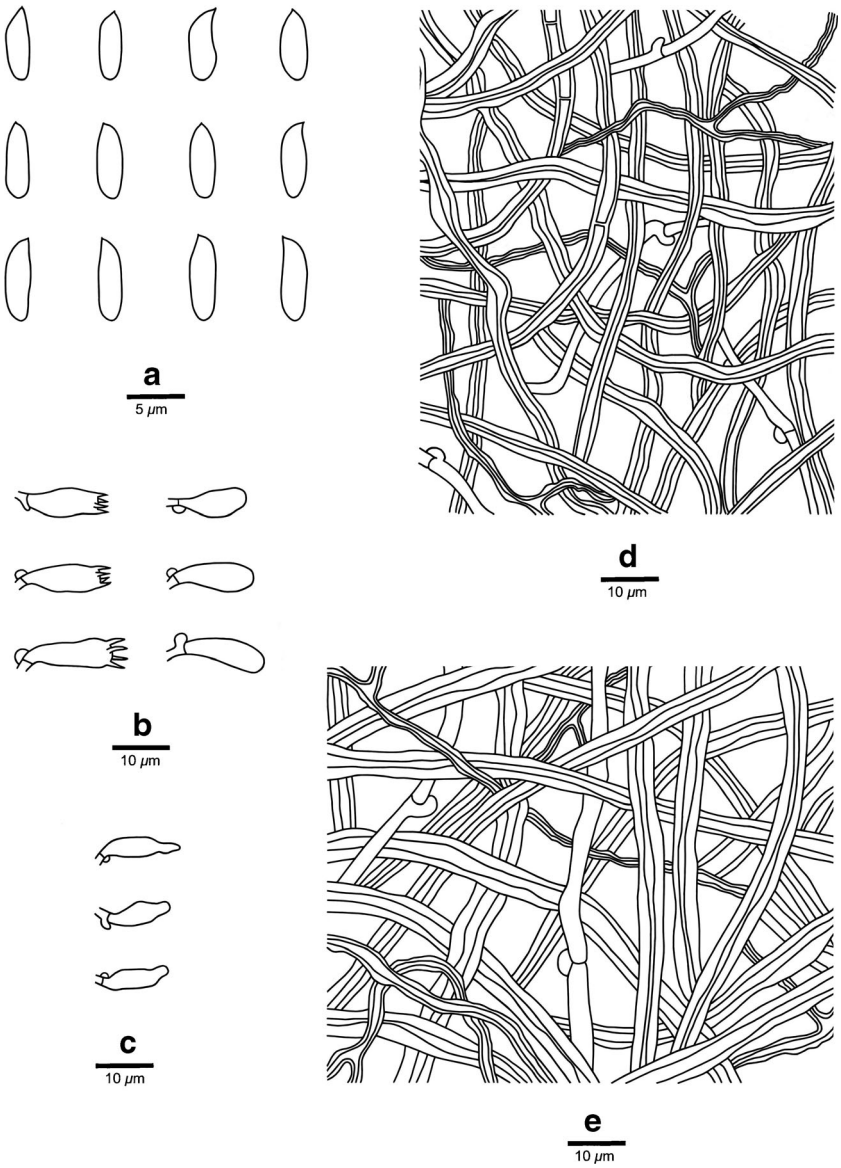

Fig. 4 Microscopic structures of *Neofomitella guangxiensis* (drawn from the holotype). **a** Basidiospores; **b** Basidia and basidioles; **c** Cystidioles; **d** Hyphae from trama; **e** Hyphae from context. Bars: **a** = 5 μm; **a**–**e** = 10 μm

1 mm wide; pores round to angular, 5–6 per mm; dissepiments thin, entire. Context straw-yellow, corky, up to 1 mm thick. Tubes concolorous with context, corky, up to 2 mm long.

Hyphal structure. Hyphal system trimitic; generative hyphae bearing clamp connections; skeletal and binding hyphae weakly dextrinoid, CB–; tissues turning to brown in KOH.

Context. Generative hyphae infrequent, hyaline, thin-walled, rarely branched, 2–3.5 μm in diam; skeletal hyphae dominant, pale yellowish brown, thick-walled with a wide to narrow lumen, rarely branched, strongly interwoven, 2–5 μm in diam; binding hyphae hyaline to pale yellowish brown, thick-walled with a narrow lumen to subsolid, flexuous, frequently branched, interwoven, 1–2.5 μm in diam.

Tubes. Generative hyphae infrequent, hyaline, thin-walled, unbranched, 1.5–3 μm in diam; skeletal hyphae dominant, pale yellowish brown, thick-walled with a narrow lumen to subsolid, rarely branched, strongly interwoven, rarely simple-septate, 2–3 μm in diam; binding hyphae hyaline to pale yellowish brown, thick-walled with a narrow lumen to subsolid, flexuous, frequently branched, interwoven, 1–2 μm in diam. Cystidia absent, fusoid cystidioles present, hyaline, thin-walled, 10.5–14.5 × 3–4 μm. Basidia clavate, bearing four sterigmata and a basal clamp connection, 13–16.5 × 4–5 μm; basidioles in shape similar to basidia, but slightly smaller.

Spores. Basidiospores cylindrical, hyaline, smooth, thin-walled, IKI–, CB–, 5.5–7.5(−8) × (1.7–)1.8–2.2(−2.4) μm, L = 6.38 μm, W = 1.99 μm, Q = 3.12–3.31 (n = 90/3).

Type of rot. White rot.

Additional specimens (paratypes) examined. China. Guangxi Auto. Reg., Longzhou County, Nonggang Nature Reserve, on fallen angiosperm branch, 4 July 2016, Cui 13968 (BJFC); Shangsi County, Shiwandashan National Forest Park, on fallen angiosperm branch, 6 July 2016, Cui 13984 & Cui 14005 (BJFC).

Discussion

In the present study, *Neofomitella australiensis* from southern Australia and *N. guangxiensis* from southern China are supported in *Neofomitella* by a combined multi-gene dataset and can be distinguished from other *Neofomitella* species by morphological characters and phylogenetic evidence.

Neofomitella australiensis is phylogenetically related to *N. fumosipora* and *N. rhodophaea* (Fig. 1), but morphologically *N. fumosipora* has grayish-red context, smaller pores (7–9 per mm; Hattori 2005) and smaller basidiospores (3–4 × 1.7–2.2 μm; Li et al. 2014). *Neofomitella rhodophaea* differs from *N. australiensis* in its oblong-ellipsoid basidiospores and absence of cystidioles (Li et al. 2014). Both *N. polyzonata* and *N. australiensis* have cystidioles and cylindrical basidiospores, but *N. polyzonata* has velutinate pileal surface, larger pores (3–4 per mm), non-dextrinoid skeletal and binding hyphae (Li et al. 2014).

Neofomitella guangxiensis and *N. fumosipora* share glabrous pileal surface, and presence of cystidioles, but *N. fumosipora* has distinct smaller pores (7–9 per mm; Hattori 2005) and basidiospores (3–4 × 1.7–2.2 μm; Li et al. 2014). *Neofomitella polyzonata* is similar to *N. guangxiensis* in producing annual basidiomata and presence of cystidioles, but *N. polyzonata* has distinctly pileate basidiomata, velutinate pileal surface, larger pores (3–4 per mm) and smaller basidiospores (3.9–5 × 1.9–2.1 μm; Li et al. 2014). Both *N. guangxiensis* and *N. rhodophaea* have glabrous pileal surface, but *N. rhodophaea* has oblong-ellipsoid basidiospores (3.5–4.5 × 2.5–3 μm) and smaller pores (7–8 per mm), and lacks cystidioles (Li et al. 2014).

Neofomitella is phylogenetically close to *Microporus*. Morphologically, they both have a trimitic hyphal system, and hyaline, thin-walled, smooth, non-dextrinoid and non-amyloid basidiospores, but *Microporus* has centrally to laterally stipitate basidiomata with white to cream context (Gilbertson and Ryvarden 1986; Núñez and Ryvarden 2001; Li et al. 2014). *Neofomitella* was derived from *Fomitella*, they both have annual to perennial and effused-reflexed to pileate basidiomata, a trimitic hyphal system, and hyaline and thin-walled basidiospores, but *Neofomitella* has distinctly crusted basidiomata with the cuticle developing from base to margin, while *Fomitella* has the cuticle that develops from the base but does not usually extend to the very margin (Hattori 2005; Li et al. 2014). *Coriolopsis strumosa* (Fr.) Ryvarden is similar to *Neofomitella* in having encrusted basidiomata with glabrous pileal surface and a trimitic hyphal system, but *C. strumosa* has olivaceous-brown context and distinctly larger basidiospores (9–12 × 3–3.7 μm; Núñez and Ryvarden 2001; Li et al. 2014).

Until now, 5 species are accepted in *Neofomitella*. An identification key to the species of *Neofomitella* is provided.

Key to species of *Neofomitella*

1 Pileal surface velutinate, pores 3–4 per mm..... ..... *N. polyzonata*
1 Pileal surface glabrous, pores 5–9 per mm..... 2
2 Cystidioles absent, basidiospores oblong-ellipsoid ..... *N. rhodophaea*
2 Cystidioles present, basidiospores cylindrical to oblong-ellipsoid..... 3
3 Pore surface dark brown when dry, pores 7–9 per mm; basidiospores cylindrical to oblong-ellipsoid..... ..... *N. fumosipora*
3 Pore surface buff, cinnamon-buff to straw-yellow when dry, pores 5–7 per mm; basidiospores cylindrical..... 4
4 Basidiomata annual, effused-reflexed to pileate, margin obtuse; basidiospores 5.5–7.5 × 1.8–2.2 μm..... ..... *N. guangxiensis*
4 Basidiomata annual to perennial, pileate, margin acute; basidiospores 3.8–4.9 × 1.8–2.3 μm..... *N. australiensis*

Acknowledgements We express our gratitude to Drs. Tom May (Royal Bot Gardens Victoria, Australia) and Yuan-Yuan Chen (Beijing Forestry University, China) for assistance during field collections.

Funding information The research is supported by the Fundamental Research Funds for the Central Universities (No. 2016ZCQ04) and the National Natural Science Foundation of China (Project No. 31670016).

References

Chen JJ, Cui BK, Zhou LW, Korhonen K, Dai YC (2015) Phylogeny, divergence time estimation, and biogeography of the genus *Heterobasidion* (Basidiomycota, Russulales). Fungal Divers 71: 185–200. https://doi.org/10.1007/s13225-014-0317-2

Felsenstein J (1985) Confidence intervals on phylogenetics: an approach using bootstrap. Evolution 39:783–791

Gilbertson RL, Ryvarden L (1986) North American polypores, vol 1. Fungiflora, Oslo

Hall TA (1999) Bioedit: a user-friendly biological sequence alignment editor and analysis program for Windows 95/98/NT. Nucleic Acids Symp Ser 41:95–98

Han ML, Chen YY, Shen LL, Song J, Vlasák J, Dai YC, Cui BK (2016) Taxonomy and phylogeny of the brown-rot fungi: *Fomitopsis* and its related genera. Fungal Divers 80:343–373. https://doi.org/10.1007/s13225-016-0364-y

Hattori T (2005) Type studies of the polypores described by E.J.H. Corner from Asia and West Pacific Areas 7. Species described in *Trametes* (1). Mycoscience 46:303–312. https://doi.org/10.1007/s10267-005-0250-z

Hibbett DS (1996) Phylogenetic evidence for horizontal transmission of group I introns in the nuclear ribosomal DNA of mushroom-forming

fungi. Mol Biol Evol 13:903–917. https://doi.org/10.1093/oxfordjournals.molbev.a025658

Katoh K, Standley DM (2013) MAFFT multiple sequence alignment software version 7: improvements in performance and usability. Mol Biol Evol 30:772–780. https://doi.org/10.1093/molbev/mst010

Li HJ, Li XC, Vlasák J, Dai YC (2014) *Neofomitella polyzonata* gen. et sp. nov., and *N. fumosipora* and *N. rhodophaea* transferred from *Fomitella*. Mycotaxon 129:7–20. https://doi.org/10.5248/129.7

Liu YL, Whelen S, Hall BD (1999) Phylogenetic relationships among Ascomycetes: evidence from an RNA polymerase II subunit. Mol Biol Evol 16:1799–1808. https://doi.org/10.1093/oxfordjournals.molbev.a026092

Maddison WP, Maddison DR (2017) Mesquite: a modular system for evolutionary analysis. Version 3.2 http://mesquiteproject.org

Matheny PB, Liu YJ, Ammirati JF, Hall BD (2002) Using RPB1 sequences to improve phylogenetic inference among mushrooms (*Inocybe*, Agaricales). Am J Bot 89:688–698. https://doi.org/10.3732/ajb.89.4.688

Núñez M, Ryvarden L (2001) East Asian polypores 2. Synop Fungorum 14:170–522

Nylander JAA (2004) MrModeltest v2. Program distributed by the author. Evolutionary Biology Centre, Uppsala University

Petersen JH (1996) Farvekort. The Danish Mycological Society's color chart Greve: Foreningen til Svampekundskabens Fremme

Posada D, Crandall KA (1998) Modeltest: testing the model of DNA substitution. Bioinformatics 14:817–818. https://doi.org/10.1093/bioinformatics/14.9.817

Rehner SA, Buckley E (2005) A *Beauveria* phylogeny inferred from nuclear ITS and EF1-alpha sequences: evidence for cryptic diversification and links to *Cordyceps teleomorphs*. Mycologia 97:84–98. https://doi.org/10.3852/mycologia.97.1.84

Ronquist F, Huelsenbeck JP (2003) Mrbayes 3: Bayesian phylogenetic inference under mixed models. Bioinformatics 19:1572–1574

Shen LL, Wang M, Zhou JL, Xing JH, Cui BK, Dai YC (2019) Taxonomy and phylogeny of *Postia*. Multi-gene phylogeny and taxonomy of the brown-rot fungi: *Postia* (Polyporales, Basidiomycota) and related genera. Persoonia 42:101–126. https://doi.org/10.3767/persoonia.2019.42.05

Song J, Cui BK (2017) Phylogeny, divergence time and historical biogeography of *Laetiporus* (*Basidiomycota*, *Polyporales*). BMC Evol Biol 17:102. https://doi.org/10.1186/s12862-017-0948-5

Song J, Chen JJ, Wang M, Chen YY, Cui BK (2016) Phylogeny and biogeography of the remarkable genus *Bondarzewia* (Basidiomycota, Russulales). Sci Rep 6(34568). https://doi.org/10.1038/srep34568

Stamatakis A (2006) RAxML-VI-HPC: maximum likelihood-based phylogenetic analyses with thousands of taxa and mixed models. Bioinformatics 22:2688–2690. https://doi.org/10.1093/bioinformatics/btl446

Swofford DL (2002) PAUP*. Phylogenetic analysis using parsimony (*and other methods). Version 4.0b10. Sinauer, Sunderland

White TJ, Bruns T, Lee S, Taylor J (1990) Amplification and direct sequencing of fungal ribosomal RNA genes for phylogenetics. In: Innis MA, Gelfand DH, Sninsky JJ, White TJ (eds) PCR protocols: a guide to methods and applications. Academic, San Diego, pp 315–322

Zhou JL, Zhu L, Chen H, Cui BK (2016) Taxonomy and phylogeny of *Polyporus* group *Melanopus* (Polyporales, Basidiomycota) from China. PLoS One 11(8):e0159495. https://doi.org/10.1371/journal.pone.0159495